Chin J Integr Med 2019 Mar;25(3):182-189

Chinese Journal of Integrative Medicine

Available online at link.springer.com/journal/11655
Journal homepage: www.cjim.cn/zxyjhen/zxyjhen/ch/index.aspx
E-mail: cjim_en@cjim.cn

Original Article

Effects of *Polygonum cuspidatum* on AMPK-FOXO3α Signaling Pathway in Rat Model of Uric Acid-Induced Renal Damage*

MA Wei-guo[1], WANG Jie[2], BU Xiang-wei[1], ZHANG Hong-hong[1], ZHANG Jian-ping[1], ZHANG Xiao-xu[1], HE Yu-xi[1], WANG Da-li[1], ZHANG Zheng-ju[1], and MENG Feng-xian[1]

ABSTRACT **Objective:** To observe the effects of Chinese medicine (CM) *Polygonum cuspidatum* (PC) on adenosine 5'-monophosphate-activated protein kinase (AMPK), forkhead box O3α (FOXO3α), Toll-like receptor-4 (TLR4), NACHT, LRR and PYD domains-containing protein 3 (NLRP3), and monocyte chemoattractant protein-1 (MCP-1) expression in a rat model of uric acid-induced renal damage and to determine the molecular mechanism. **Methods:** A rat model of uric acid-induced renal damage was established, and rats were randomly divided into a model group, a positive drug group, and high-, medium-, and low-dose PC groups (n=12 per group). A normal group (n=6) was used as the control. Rats in the normal and model groups were administered distilled water (10 mL•kg^{-1}) by intragastric infusion. Rats in the positive drug group and the high-, medium-, and low-dose PC groups were administered allopurinol (23.33 mg•kg^{-1}), and 7.46, 3.73, or 1.87 g•kg^{-1}•d^{-1} PC by intragastric infusion, respectively for 6 to 8 weeks. After the intervention, reverse transcription polymerase chain reaction, Western blot, enzyme linked immunosorbent assay, and immunohistochemistry were used to detect AMPK, FOXO3α, TLR4, NLRP3, and MCP-1 mRNA and protein levels in renal tissue or serum. **Results:** Compared with the normal group, the mRNA transcription levels of AMPK and FOXO3α in the model group were significantly down-regulated, and protein levels of AMPKα1, pAMPKα1 and FOXO3α were significantly down-regulated at the 6th and 8th weeks (P<0.01 or P<0.05). The mRNA transcription and protein levels of TLR4, NLRP3 and MCP-1 were significantly up-regulated (P<0.01 or P<0.05). Compared with the model group, at the 6th week, the mRNA transcription levels of AMPK in the high- and medium-dose groups, and protein expression levels of AMPKα1, pAMPKα1 and FOXO3α in the high-dose PC group, AMPKα1 and pAMPKα1 in the medium-dose PC group, and pAMPKα1 in the low-dose PC group were significantly up-regulated (P<0.01 or P<0.05); the mRNA transcription and protein levels of TLR4 and NLRP3 in the 3 CM groups, and protein expression levels of MCP-1 in the medium- and low-dose PC groups were down-regulated (P<0.01 or P<0.05). At the 8th week, the mRNA transcription levels of AMPK in the high-dose PC group and FOXO3α in the medium-dose PC group, and protein levels of AMPKα1, pAMPKα1 and FOXO3α in the 3 CM groups were significantly up-regulated (P<0.01 or P<0.05); the mRNA transcription levels of TLR4 in the medium- and low-dose PC groups, NLRP3 in the high- and low-dose PC groups and MCP-1 in the medium- and low-dose PC groups, and protein expression levels of TLR4, NLRP3 and MCP-1 in the 3 CM groups were down-regulated (P<0.01 or P<0.05). **Conclusion:** PC up-regulated the expression of AMPK and its downstream molecule FOXO3α and inhibited the biological activity of TLR4, NLRP3, and MCP-1, key signal molecules in the immunoinflammatory network pathway, which may be the molecular mechanism of PC to improve hyperuricemia-mediated immunoinflammatory metabolic renal damage.

KEYWORDS *Polygonum cuspidatum*, Chinese medicine, uric acid, renal damage, AMPK-FOXO3α pathway

Primary hyperuricemia is a polygenic disease characterized by purine metabolic disorders and excessive production or reduced excretion of uric acid. The disease can result in multi-organ injuries

*Supported by the National Natural Science Foundation of China (No. 81473516 and No. 30973918)
1. Department of Rheumatology, Dongfang Hospital, Beijing University of Chinese Medicine, Beijing (100078), China; 2. Department of Endocrinology, Shunyi Branch, Beijing Hospital of Traditional Chinese Medicine, Beijing (101300), China
Correspondence to: Prof. MENG Feng-xian, Tel: 86-10-67689721, E-mail: mfx0823@163.com
DOI: https://doi.org/10.1007/s11655-017-2979-6

and due to a high incidence, complex mechanisms, and treatment limitations, it is a difficult problem facing the international medical community. The kidneys are the main organ for uric acid metabolism. The high number of uric acid crystals excreted via the kidneys directly mediate and participate in the development of renal damage. In addition, hyperuricemia can over-activate both the renal renin-angiotensin system and endothelin, resulting in glomerular hypertension, damaging renal arteriole endothelial cell functions, and stimulating vascular smooth muscle cell proliferation. These processes can lead to glomerular afferent arteriole wall hardening and thickening, causing secondary renal tubular interstitial inflammation and fibrosis.[1,2] Hyperuricemia, an independent risk factor for renal disease, can also result in glomerular hypertrophy and mesangial cell proliferation.[3-5]

The pathogenesis of uric acid nephropathy is multifactorial. However, there are few studies on this topic. In the current study, a rat model of renal damage induced by hyperuricemia was established, and the effects of *Polygonum cuspidatum* (PC) on the biological functions of 5'-monophesphate-activated protein kinase (AMPK) were observed and the mechanisms were determined.

METHODS

Animals

Healthy specific-pathogen-free male Sprague Dawley rats weighing 190–210 g were provided by Beijing Vital River Laboratory Animal Technology [certificate No. SCXK (Beijing) 2012-0001]. Yeast feed was provided by Beijing HFK Bioscience [certificate No. SCXK (Beijing) 2014-0008].

Drugs, Reagents and Instruments

Chinese medicine (CM) PC decoction was provided at 40 g/25 mL per bag by the Department of Pharmacy, Dongfang Hospital, Beijing University of Chinese Medicine and stored at 4 ℃ in a refrigerator until use. Allopurinol capsule was provided at 0.25 g/tablet (a total of 10 tablets) by Heilongjiang AolidaNaide Pharmaceutical, China (batch No. 15010901).

Adenine (batch No. A8626) and sodium carboxymethyl cellulose (batch No. 21902) were from Sigma-Aldrich (St. Louis, MO, USA); the rat monocyte chemoattractant protein-1 (MCP-1) enzyme linked immunosorbent assay (ELISA) kit (batch No. M1752164) was from Neobioscience, China; anti-AMPK α 1 antibody (batch No. ab32047), anti-pAMPK α 1 antibody (batch No. ab131357), and anti-TLR4 antibody (batch No. ab13556) were from Abcam; anti-FOXO3 α antibody (batch No. 12829S) and anti-NLRP3 antibody (batch No. 15101) were from CST Company, USA; a THiF iScript cDNA first strand synthetic kit (batch No. CW2569) was from Beijing ComWin Biotech, China; and SYBR FAST qPCR Kit Master Mix (2 ×) (batch No. KK4610) was from KAPA Biosystems, USA.

Instruments used were a HC-3018R high-speed freezing centrifuge (Anhui USTC Zonkia Scientific Instruments, China); a 5810R desktop freezing centrifuge (Eppendorf, Germany); JY300C electrophoresis apparatus and electrophoresis tank, JY-2Y1 transfer film instrument (Beijing JUNYI Electrophoresis, China); ChampGel5000 gel imager (Beijing Sage Creation Science, China); SMA-1000 spectrophotometer (Merinton Instrument, Inc.); StepOne Plus real-time quantitative PCR instrument (ABI); TC-96/G/H(b) gradient PCR instrument (Hangzhou Bioer Technology, China); AR1140 animal organ electronic balance (Chaus, USA); Shandon Excelsior ES automatic dewatering machine, China; Shandon Exciso ES automatic dewatering machine, China; Shandon Histocentre 3 paraffin embedding machine, China; Shandon Finesse 325 rotary microtome, China; MULTISKAN MK3 fully automatic multifunctional microplate reader (Thermo, USA); and a X71 automatic optical photographic microscope (Olympus, Japan).

Modeling, Grouping, and Intervention

Rats had free access to water and food. After being allowed to acclimatize for 1 week, rats were randomly divided into a normal group (n=6) and a model group (n=99). The normal group was administered distilled water at 10 mL•kg^{-1}•d^{-1} by intragastric infusion and fed a normal diet. In the modeling groups, adenine was dissolved in 0.5% sodium carboxymethyl cellulose solution, and was administered at 100 mg•kg^{-1}•d^{-1} by intragastric infusion, and 10% yeast feed was given at 100 g•kg^{-1}•d^{-1} for 18 consecutive days.

Blood was taken from the orbital canthus and the serum uric acid level was found to be higher than 82.50 μmol/L, which was significantly different from the normal group at the same time (P<0.05),

and was deemed to be successful development of a rat hyperuricemia model.[6] Urine was collected from model rats housed in metabolic cage for 24 h. The concentration of urinary protein was found to be significantly higher than the normal group, and was indicative of renal damage, confirming uric acid renal damage.

Totally 60 model rats were divided into a model group, a positive drug group, and high-, medium-, and low-dose of PC groups (CM groups) through a table of random numbers, 12 in each group. The normal and model groups were administered distilled water (10 mL•kg^{-1}) daily by intragastric infusion. The positive drug group and the high-, medium-, and low-dose CM groups were administered 23.33 mg•kg^{-1} of zyloprim, and 7.46, 3.73, and 1.87 g•kg^{-1} PC, respectively, daily by intragastric infusion. The doses of zyloprim and the high-, medium-, and low-dose PC were the equivalent of 5.6-, 11.2-, 5.6-, and 2.8-times per kg of body weight of adults, respectively. Interventions lasted for 6 to 8 weeks.

Specimen Collection

After 6- and 8-week intragastric infusion, half the rats in each group were randomly selected and blood was taken from the abdominal aorta after anesthesia by intraperitoneal injection of pentobarbital sodium (40 mg•kg^{-1}). Blood was centrifuged and the supernatant was collected and stored at –80 ℃ for ELISA and biochemical indicator detection. Following blood collection, the rats were sacrificed, the kidneys were removed. The left kidney was cut length-wise along the lateral margin. One half of the segmented kidney was fixed with 10% neutral formalin solution for immunohistochemistry and light microscopy and the other half was fixed with 2.5% glutaraldehyde solution for electron microscopy. The right kidney was frozen and stored in liquid nitrogen for later analyses with reverse transcription polymerase chain reaction (RT-PCR) and Western blot. One rat in the low-dose CM group died at week 8 following failed intragastric infusion.

Indicator Detection and Methods

RT-PCR was used to detect AMPK, FOXO3α, TLR4 NLRP3, and MCP-1 gene transcription levels in renal tissue, and Western blot and immunohistochemistry were used to detect AMPKα1, pAMPKα1, FOXO3α, TLR4, and NLRP3 protein in renal tissue. ELISA was used to detect serum MCP-1 protein levels.

For RT-PCR, 100 mg renal tissue was subject to TriZol extraction of RNA for reverse transcription to obtain cDNA before real-time fluorescence quantification PCR was conducted. For PCR, the reaction volume was 10 μL and contained SYBR FAST qPCR Kit Master Mix (2×) 5 μL + upstream primer (10 μmol/L) 0.2 μL + downstream primer (10 μmol/L) 0.2 μL + cDNA 1 μL + nuclease-free ultrapure water (3.6 μL). Reaction conditions were pre-denaturation at 95 ℃ for 5 min, denaturation at 95 ℃ for 10 s, annealing for 5 s, and extension at 60 ℃ for 34 s for 40 cycles. Dissolution curve analysis was conducted to identify the specificity of the PCR product. Sequence Detection System software was used to analyze cycle threshold values for each specimen of PCR. Primer design and synthesis are shown in Table 1.

Table 1. Primer Design for cDNA Synthesis

Gene	Primer sequence	Length (bp)
AMPKα1	U: 5'-CTTCTTAACTCCTCCCCTCCAC-3'	140
	D: 5'-CTAAATCAGGTTACTCTGGGCAA-3'	
FOXO3α	U: 5'-GGAAAGGGGAAATGGGCAAA-3'	131
	D: 5'-GGGAGTCACAAAGGTGTCAAGC-3'	
TLR4	U: 5'-AAAGGAACATCATTCTTCTCTGGA-3'	116
	D: 5'-GGGAAAGGAAGGAAACATTCACT-3'	
NLRP3	U: 5'-ACTGTAAGCTACAGATGCTGGAGTT-3'	124
	D: 5'-AGGTCGTTGTTGCTCAAGTTCA-3'	
MCP-1	U: 5'-GGTGTCCCAAAGAAGCTGTAGTATT-3'	115
	D: 5'-CTCACTTGGTTCTGGTCCAGTTT-3'	
ACTB	U: 5'-GCACCATGAAGATCAAGATCATT-3'	172
	D: 5'-TAACAGTCCGCCTAGAAGCATT-3'	

Notes: U: upstream; D: downstream

For Western blot, 100 mg renal tissue was added to 1 mL protein extraction reagent and inhibitor and then mixed for full cleavage. After centrifugation, the supernatant was collected and the protein concentration was measured using a bicinchoninic acid assay kit. Sample protein concentrations were adjusted to the same level, loaded with sample buffer, and underwent denaturation at 95 ℃ for 5 min before being stored for later use. SDS polypropylene gel electrophoresis was conducted using 8%, 10%, and 12% separation gels and a 5% spacer gel. Electrophoresis using the spacer gel was conducted at 90 V and the separation gels at 120 V. Electrophoresis was terminated when bromophenol blue ran to the end of the gel. A wet transfer to the membrane was

conducted for 90 min. The PVDF membrane was blocked with blocking solution containing 5% skimmed milk powder. The primary antibody was diluted and incubated with the membrane overnight at 4 ℃. A secondary horseradish peroxidase-labeled antibody was diluted at a ratio of 1:10000 and incubated with the membrane for 40 min. Electrochemiluminescence was conducted. A gel image analysis system was used to scan protein bands, and Image system (ver. 4.00) software was used to analyze gradation of the image. The change in the relative content was equal to the target protein gray level/β-actin gray level.

ELISA was performed according to the manufacturer's instructions.

For immunohistochemistry, tissue sections were dewaxed and washed. The antigen was retrieved through high-pressure heating. Endogenous peroxidase activity was blocked with hydrogen peroxide. The non-specific antigen was blocked with goat serum. The primary antibody was incubated overnight at 4 ℃. The secondary antibody was incubated at 37 ℃ for 10–15 min in horseradish enzyme-labeled streptavidin working solution. 3,3'-Diaminobenzidine coloration and hematoxylin counterstaining were performedbefore sections were sealed in neutral resin. Using microscopy, brown particles in the cytoplasm were identified as positive and non-stained areas as negative. Three visual fields were randomly selected from the positive expression area of each section. The IPP6.0 true color image analysis system was used to determine average integral optical density (IOD) values of positive expression areas in the three visual fields.

Statistical Methods

SPSS 22.0 statistical software was used for analyses. Data were expressed as mean ± standard deviation ($\bar{x} \pm s$). One-way analysis of variance was used for multi-group comparisons. In cases of equal variance, the least significant difference test was used for comparisons between two groups. In cases of heterogeneity of variance, the Tamhane's T2 test was used. A *P*-value <0.05 was considered statistically significant.

RESULTS

AMPK, FOXO3α, TLR4, NLRP3, and MCP-1 mRNA Transcription Levels in Renal Tissue

Compared with the normal group, at week 6, mRNA transcription levels of AMPK in the model group were significantly down-regulated and TLR4 and NLRP3 were significantly up-regulated (*P*<0.01). At week 8, mRNA transcription levels of AMPK and FOXO3α were significantly down-regulated and TLR4, NLRP3, and MCP-1 were significantly up-regulated, respectively (*P*<0.01 or *P*<0.05). Compared with the model group, at week 6, mRNA transcription levels of AMPK in the high- and medium-dose PC groups were significantly up-regulated, TLR4 and NLRP3 in the 3 CM groups were significantly down-regulated (*P*<0.01 or *P*<0.05). At week 8, mRNA transcription levels of AMPK in the high-dose PC group were significantly up-regulated, TLR4 in the medium- and low-dose PC groups, NLRP3 in the high- and low-dose PC groups, and MCP-1 in the medium- and low-dose PC groups were significantly down-regulated (*P*<0.01), FOXO3α in the medium-dose PC group was significantly up-regulated (*P*<0.05, Table 1).

AMPKα1, pAMPKα1, FOXO3α, TLR4, and NLRP3 Protein Levels in Renal Tissue

Compared with the normal group, protein expression levels of AMPKα1, pAMPKα1, and FOXO3α were significantly down-regulated and protein expression levels of TLR4 and NLRP3 were significantly up-regulated in the model group at weeks 6 and 8 (*P*<0.01). Compared with the model group, AMPKα1, pAMPKα1 and FOXO3α protein expression levels were all up-regulated at weeks 6 and 8 (*P*<0.05 or *P*<0.01), except for AMPKα1 in the low- and high-dose PC groups and FOXO3α in the medium- and low-dose PC groups at week 6. TLR4 and NLRP3 protein expression levels in the 3 CM groups were all down-regulated compared with the model group at weeks 6 and 8 (*P*<0.05 or *P*<0.01; Table 2, Figure 1).

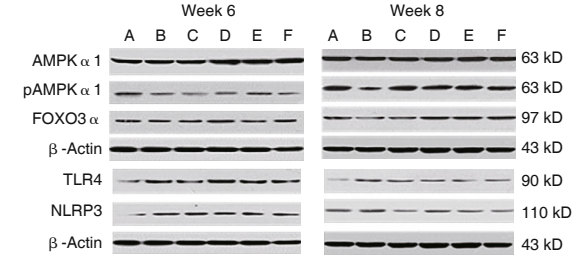

Figure 1. Western Blot of AMPKα1, pAMPKα1, FOXO3α, TLR4, NLRP3 in Renal Tissue of Rats

Notes: A: normal group; B: model group; C: positive drug group; D: high-dose PC group; E: medium-dose PC group; F: low-dose PC group

Chin J Integr Med 2019 Mar;25(3):182-189

Table 1. mRNA Transcription Levels of AMPK, FOXO3α, TLR4, NLRP3 and MCP-1 in Renal Tissue of Rats at the 6th and 8th Weeks by RT-PCR ($\bar{x} \pm s$)

Group	Week	*n*	AMPK	FOXO3α	TLR4	NLRP3	MCP-1
Normal	6	3	0.13±0.03	1.16±0.60	0.48±0.05	1.12±0.11	0.73±0.24
	8	3	0.06±0.00	0.87±0.03	0.35±0.05	1.94±0.68	0.58±0.11
Model	6	6	0.04±0.00**	0.79±0.06	1.57±0.24**	4.52±1.01**	2.07±1.23
	8	6	0.04±0.00**	0.65±0.00**	0.84±0.15*	4.79±0.43*	2.10±0.38*
Positive drug	6	6	0.09±0.02$^{\triangle}$	1.31±0.33	0.44±0.09$^{\triangle\triangle}$	4.08±0.57	0.61±0.19
	8	6	0.04±0.00$^{\triangle}$	1.54±0.30$^{\triangle}$	0.35±0.09$^{\triangle\triangle}$	4.81±1.03	1.20±0.24$^{\triangle\triangle}$
High-dose PC	6	6	0.14±0.01$^{\triangle\triangle}$	0.90±0.11	0.50±0.22$^{\triangle\triangle}$	1.67±0.40$^{\triangle}$	2.22±1.43
	8	6	0.19±0.03$^{\triangle\triangle}$	0.85±0.16	0.51±0.28	1.86±1.14$^{\triangle}$	1.40±0.63
Medium-dose PC	6	6	0.11±0.03$^{\triangle}$	0.82±0.01	0.78±0.34$^{\triangle\triangle}$	2.03±0.39$^{\triangle}$	1.22±0.59
	8	6	0.04±0.01	1.19±0.15$^{\triangle}$	0.32±0.08$^{\triangle\triangle}$	2.97±0.98	0.68±0.21$^{\triangle\triangle}$
Low-dose PC	6	6	0.08±0.02	0.87±0.55	0.58±0.32$^{\triangle\triangle}$	1.77±0.73$^{\triangle}$	1.14±0.62
	8	5	0.08±0.04	0.76±0.05	0.37±0.19$^{\triangle}$	1.73±0.65$^{\triangle\triangle}$	0.82±0.07$^{\triangle\triangle}$

Notes: $^{*}P<0.05$, $^{**}P<0.01$ *vs*. normal group; $^{\triangle}P<0.05$, $^{\triangle\triangle}P<0.01$ *vs*. model group

Table 2. Protein Expression Levels of AMPKα1, pAMPKα1, FOXO3α, TLR4 and NLRP3 in Renal Tissue of Rats at the 6th and 8th Weeks by Western Blot ($\bar{x} \pm s$)

Group	Week	*n*	AMPKα1	pAMPKα1	FOXO3α	TLR4	NLRP3
Normal	6	3	0.68±0.06	0.48±0.01	0.41±0.09	0.18±0.06	0.14±0.02
	8	3	0.56±0.01	0.48±0.07	0.38±0.04	0.16±0.02	0.20±0.07
Model	6	6	0.50±0.06*	0.10±0.08*	0.18±0.06*	0.57±0.10*	0.53±0.05*
	8	6	0.42±0.05*	0.09±0.03*	0.13±0.04*	0.45±0.02*	0.50±0.04*
Positive drug	6	6	0.66±0.09	0.24±0.06$^{\triangle}$	0.33±0.04$^{\triangle}$	0.26±0.06$^{\triangle\triangle}$	0.23±0.03$^{\triangle\triangle}$
	8	6	0.58±0.04$^{\triangle\triangle}$	0.36±0.06$^{\triangle\triangle}$	0.34±0.08$^{\triangle\triangle}$	0.24±0.06$^{\triangle\triangle}$	0.23±0.01$^{\triangle\triangle}$
High-dose PC	6	6	0.65±0.10	0.41±0.04$^{\triangle\triangle}$	0.40±0.10$^{\triangle}$	0.29±0.09$^{\triangle}$	0.23±0.04$^{\triangle\triangle}$
	8	6	0.49±0.02$^{\triangle}$	0.36±0.02$^{\triangle\triangle}$	0.33±0.04$^{\triangle\triangle}$	0.20±0.06$^{\triangle\triangle}$	0.27±0.05$^{\triangle\triangle}$
Medium-dose PC	6	6	0.70±0.04$^{\triangle\triangle}$	0.36±0.10$^{\triangle}$	0.40±0.17	0.30±0.02$^{\triangle\triangle}$	0.19±0.01$^{\triangle\triangle}$
	8	6	0.56±0.05$^{\triangle}$	0.36±0.09$^{\triangle\triangle}$	0.34±0.04$^{\triangle\triangle}$	0.25±0.03$^{\triangle\triangle}$	0.32±0.10$^{\triangle}$
Low-dose PC	6	6	0.66±0.07	0.38±0.01$^{\triangle\triangle}$	0.30±0.12	0.26±0.06$^{\triangle\triangle}$	0.29±0.00$^{\triangle\triangle}$
	8	5	0.55±0.03$^{\triangle\triangle}$	0.41±0.07$^{\triangle\triangle}$	0.31±0.04$^{\triangle\triangle}$	0.24±0.08$^{\triangle\triangle}$	0.32±0.04$^{\triangle\triangle}$

Notes: $^{*}P<0.01$ *vs*. normal group; $^{\triangle}P<0.05$, $^{\triangle\triangle}P<0.01$ *vs*. model group

MCP-1 Protein Expression Level in Serum

Compared with the normal group, protein expression levels of MCP-1 were significantly up-regulated in the model group at weeks 6 and 8 ($P<0.05$). Compared with the model group, protein expression levels of MCP-1 in the medium- and low-dose PC groups were significantly down-regulated at week 6 and in the 3 CM groups at week 8 were significantly down-regulated ($P<0.05$ or $P<0.01$, Table 3).

Table 3. Protein Expression Levels of MCP-1 in Rats' Serum at the 6th and 8th Weeks by ELISA (ng/L, $\bar{x} \pm s$)

Group	*n*	Week 6	*n*	Week 8
Normal	3	92.53±33.80	3	56.35±42.08
Model	6	183.57±5.92*	6	192.53±40.48*
Positive drug	6	102.47±46.76$^{\triangle}$	6	62.14±29.52$^{\triangle}$
High-dose PC	6	106.04±81.67	6	71.01±44.65$^{\triangle}$
Medium-dose PC	6	130.37±43.98$^{\triangle}$	6	80.04±47.11$^{\triangle}$
Low-dose PC	6	129.55±14.98$^{\triangle\triangle}$	5	83.30±29.67$^{\triangle}$

Notes: $^{*}P<0.05$ *vs*. normal group; $^{\triangle}P<0.05$, $^{\triangle\triangle}P<0.01$ *vs*. model group

Average IOD Test Results for AMPKα1, pAMPKα1, FOXO3α, TLR4, and NLRP3 in Renal Tissue

Compared with the normal group, AMPKα1 and pAMPKα1 were significantly down-regulated in the model group at week 6, NLRP3 was significantly up-regulated ($P<0.01$), and FOXO3α was significantly down-regulated ($P<0.05$). At week 8, pAMPKα1 and FOXO3α were significantly down-regulated, TLR4 and NLRP3 were significantly up-regulated ($P<0.05$ or

Table 4. Average IOD of AMPK α 1, pAMPK α 1, FOXO3 α, TLR4 and NLRP3 in Renal Tissue of Rats at the 6th and 8th Weeks ($\bar{x} \pm s$)

Group	Week	*n*	AMPK α 1	pAMPK α 1	FOXO3 α	TLR4	NLRP3
Normal	6	3	69.49 ± 9.59	66.60 ± 11.60	231.27 ± 19.28	70.80 ± 7.66	40.04 ± 2.82
	8	3	57.91 ± 9.77	62.16 ± 8.75	214.10 ± 34.84	67.41 ± 5.50	46.23 ± 5.27
Model	6	6	47.84 ± 9.39**	44.08 ± 8.15**	192.56 ± 23.65*	82.30 ± 10.33	67.41 ± 6.96**
	8	6	51.14 ± 10.00	40.02 ± 7.98**	169.91 ± 27.19*	87.05 ± 8.09**	67.43 ± 7.30**
Positive drug	6	6	63.95 ± 7.14$^{△△}$	54.95 ± 8.65$^{△}$	211.96 ± 16.16	70.82 ± 7.65	57.92 ± 4.70$^{△}$
	8	6	55.59 ± 12.14	51.32 ± 5.75$^{△}$	207.20 ± 22.08$^{△}$	76.42 ± 5.36$^{△}$	51.99 ± 7.64$^{△△}$
High-dose PC	6	6	59.96 ± 9.37$^{△}$	56.22 ± 8.77$^{△}$	205.86 ± 13.46	73.18 ± 9.42	64.52 ± 4.22
	8	6	51.40 ± 7.86	58.12 ± 10.33$^{△△}$	212.84 ± 27.89$^{△}$	70.19 ± 4.16$^{△△}$	55.39 ± 4.21$^{△△}$
Medium-dose PC	6	6	58.35 ± 8.36	58.60 ± 11.86$^{△}$	196.31 ± 23.48	75.54 ± 3.48	61.23 ± 6.61
	8	6	57.68 ± 12.43	55.91 ± 7.80$^{△△}$	206.83 ± 28.67$^{△}$	74.91 ± 6.99$^{△}$	53.77 ± 6.30$^{△△}$
Low-dose PC	6	6	50.03 ± 7.01	54.90 ± 13.60	188.08 ± 42.48	80.68 ± 8.62	66.60 ± 7.70
	8	5	54.55 ± 11.52	54.93 ± 10.77$^{△}$	201.28 ± 25.71	76.73 ± 5.86$^{△}$	49.77 ± 4.43$^{△△}$

Notes: $^{*}P<0.05$, $^{**}P<0.01$ *vs*. normal group; $^{△}P<0.05$, $^{△△}P<0.01$ *vs*. model group

P<0.01). Compared with the model group, the average IOD levels of AMPK α 1 in the high-dose PC group and pAMPK α 1 in the high- and medium-dose PC groups at week 6, and pAMPK α 1 in 3 CM groups and FOXO3 α in the high- and medium-dose PC groups at week 8 were all up-regulated (*P*<0.05 or *P*<0.01); IOD levels of TLR4 and NLRP3 at week 8 were all down-regulated (*P*<0.05 or *P*<0.01; Table 4, Appendix 1).

DISCUSSION

In hyperuricemia, molecular level studies have identified that the TLR-mediated immune signaling pathway and the novel cryopyrin inflammatory signaling pathway were activated by urate stimuli. TLR is a type Ⅰ transmembrane protein and is the major pattern recognition receptor of the innate immune system. TLR is the only known major transmembrane protein in mammals that transmits extracellular antigen recognition information into cells, resulting in inflammatory responses.[7] Combinations of TLR and corresponding ligands result in a series of protein cascade reactions that activate nuclear factor (NF-κB) and JUN/FOS to induce the activation of many rapid response genes and produce effector molecules that participate in inflammatory responses. TLR4 plays a dominant role in mediating inflammatory response signal transduction. TLR4 induces and activates NF-κB via the connexin MyD88-dependent or non-dependent signaling pathways, the well-known TLR4/NF-κB inflammatory pathway. This pathway participates in the development of the microinflammatory state of renal impairment,[8] and mediates the occurrence and development of renal interstitial fibrosis. Studies suggest that after activating leukocytes, urate activates inflammatory factors through TLR2 and TLR4 in the innate immune system, and then activates interleukin (IL)-1, resulting in inflammatory effects and tissue damage.[9] The results of the current study suggest that the therapeutic agent tested effectively down-regulated transcription and protein expression of TLR4. The TLR4 pathway is a core component in hyperuricemia-mediated renal damage. The cryopyrin inflammasome, also known as NALP3, NLRP3, CLAS or PYPAF1, is mainly expressed in neutrophilic granulocytes, mononuclear macrophages, and some primary immune cells.[10] In the current study, examination of the expression of NLRP3 suggested that NLRP3 and TLR4 were in the active expression state when hyperuricemia mediates immunoinflammatory renal tissue injury.

The glomerular MCP-1 expression level is associated with the degree of glomerular damage, and MCP-1 locally produced by the renal interstitium is also involved in tubular interstitial damage.[8] MCP-1 can act on renal tubular epithelial cells, activate NF-κB and AP-1, and increase IL-6 and intercellular adhesion molecule 1 expression. Urate depositions in the kidney directly stimulate increases in MCP-1 protein expression in renal tissue and induces activation of inflammatory factors by activating NF-κB, causing renal vascular inflammatory responses and macrophage infiltration,[11] and promotes renal interstitial fibrosis. In the current study, MCP-1 expression was suggestive of the above described mechanisms.

FOXO3 α is a member of the fork head box

protein family of transcription factors. Recent studies suggested that it played an important role in inhibition of the inflammatory response.[12,13] FOXO3α may also be involved in the regulation of inflammatory responses by modulating the number and function of mononuclear macrophages or inhibiting over-activation of mononuclear macrophages.[14] Studies have reported that FOXO3α gene deletion leads to inflammatory cell infiltration of the organs including the spleen and lungs in mice. FOXO3α-deficient mice show significantly increased NF-κB activation, and compared with wild-type mice, Th1 and Th2 inflammatory factor secretion is elevated.[15] When stimulated with a High-dose of lipopolysaccharide, expression of FOXO3α in inflammatory cells decreased sharply. FOXO3α is also a downstream molecule of the P13K/Akt signaling pathway.[16] Phosphorylation and activation of P13K/Akt by inflammatory signals induces Akt to combine with FOXO3α in the nucleus, resulting in phosphorylation. Phosphorylated FOXO3α is isolated from the bonding point on DNA, and is removed from the nucleus and enters cytoplasm, thereby reducing its transcriptional activity and blocking TLR4 signaling pathway transduction.[17] In pathogen-activated antigenpresenting cells, FOXO3α can inhibit the production of inflammatory cytokines such as TNF-α and IL-6.[18] Therefore, FOXO3α has important biological effects on the regulation of immune-mediated inflammation.

Over the years, discovery of the structural characteristics and AMPK sequence at the genetic level has directed the attention of researchers on the downstream targets of AMPK from traditional enzymes participating in metabolic process to gene expression regulation and related biological processes. When AMPK is activated, phosphorylated downstream signaling molecules produce numerous biological functions. For energy metabolism transduction, AMPK has a multi-link regulatory mechanism involving glucose and lipid metabolism, specific regulatory effects on adipocytokines, and an inhibitory effect on genetic transcription of inflammatory mediators. AMPK also negatively regulates genetic transcription of inflammatory factors and inhibits cascade expansion of immunoinflammatory responses by inhibiting excessive activation and autophagy of inflammatory factors. The biological functions of AMPK, on the one hand, act as an inhibitor; AMPK is directly or indirectly involved in the negative regulation of inflammatory factors, inhibits the key transcription factors NF-κB, inducible nitric oxide synthases, and mitogen-activated protein kinases, and regulates reactive oxygen species. On the other hand, AMPK increases the activity of anti-inflammatory signal systems *in vivo* by acting as an agonist. For example, aminoimidazole-4-carboxamide ribonucleotide can reduce TNF-α, IL-1β, IL-6, and iNOS expression of peritoneal macrophages and microglial cells in rats that are induced by lipopolysaccharide. AMPK can also indirectly regulate NF-κB activity and inhibit expression of inflammatory factors by downstream sirtuin 1, FOXO3α, p53, peroxisome proliferator-activated receptor-gamma coactivator-1 alpha, and other proteins.[19] Recent studies show that AMPK directly phosphorylates FOXO3α at six regulatory sites (thr199, ser399, ser413, ser355, ser588, and ser626) and increase transcriptional activity.[15] FOXO3α may be another target on which AMPK has an anti-inflammatory effect. The biological activity of AMPK is significant in regulating energy metabolism and inhibiting immunoinflammatory reactions, and metabolic regulation is partly responsible for inhibiting the inflammatory response. It is thought that AMPK may be the regulatory molecule that contributes the most to uric acid renal damage. This idea requires further study.

The results of the current study suggest that PC (which acts to clear heat, remove dampness, and disperse toxins and blood stasis) significantly up-regulates transcription and expression of AMPK and FOXO3α in the renal tissue of rats. This has the effect of inhibiting the biological activity of TLR4, NLRP3, and MCP-1, key signaling molecules in the immunoinflammatory network pathway. PC also appears to have significant dose- and time-dependent effects. It is hypothesized that the molecular mechanism behind the ability of PC to improve hyperuricemia-mediated renal immunoinflammatory metabolic damage is associated with its regulation of the AMPK-FOXO3α signaling pathway.

Further research is required to determine the mechanisms that exert positive control on AMPK and downstream signaling molecule expression with administration of the drug allopurinol, if there is any association between allopurinol and xanthine as well as hypoxanthine and adenosine triphosphate (ATP)/adenosine monophosphate (AMP)/AMPK, if so, determination of the regulatory mechanism, and, if not, the reason for the positive test results in the current study.

Conflict of Interest

The authors declare that they have no conflicts of interest concerning this article.

Author Contributions

Meng FX contributed to the conception and design of this study. Ma WG, Wang J and Bu XW were responsible for writing the first draft and the manuscript preparation. Zhang HH, Zhang JP and Zhang XX performed the data analysis and revised the manuscript. He YX, Wang DL, and Zhang ZJ participated in carrying out the pharmacological experiments and the data collection.

Electronic Supplementary Material: Supplementary material (Appendix 1) is available in the online version of this article at https://doi.org/10.1007/s11655-017-2979-6.

REFERENCES

1. Sánchezlozada LG, Tapia E, Santamaría J, Avilacasado C, Soto V, Nepomuceno T, et al. Mild hyperuricemia induces vasoconstriction and maintains glomerular hypertension in normal and remnant kidney rats. Kidney Int 2005;67:237-247.
2. Mazzali M, Kanellis J, Han L, Feng L, Xia YY, Chen Q, et al Hyperuricemia induces a primary renal arteriolopathy in rats by a blood pressure-independent mechanism. Am J Physiol Renal Physiol 2002;282: F991-F997.
3. Albertoni G, Maquigussa E, Pessoa E, Barreto JA, Borges F, Schor N. Soluble uric acid increases intracellular calcium through an angiotensin Ⅱ-dependent mechanism in immortalized human mesangial cells. Exp Biol Med 2010;235:825-832.
4. Curhan GC, Mitch WE. Diet and kidney disease. In: Brener BM, ed. The Kidney. 8th ed. Philadelphia: Saunders Elsevier; 2008:1827-1847.
5. Zhang YK, Shen YP. Controversy and progress in the treatment of hyperuricemia in chronic kidney disease. Chin J Nephrol (Chin) 2011;27(2):75-76.
6. Wang DP, Zeng L,Shang SC, eds. Laboratory animal blood physiological and biochemical reference manual. Beijing: Science Press; 2011:129.
7. Gordon S. Pattern recognition receptors: doubling up for the innate immune response. Cell 2002;111:927-930.
8. Wolfs TG, Buurman WA, van Schadewijk A, de Vries B, Daemen MA, Hiemstra PS, et al. *In vivo* expression of Toll-like receptor 2 and 4 by renal epithelial cells: IFN-gamma and TNF-alpha mediated up-regulation during inflammation. J Immunol 2002;168:1286-1293.
9. So A. Recent advances in the pathophysiology of hyperuricemia and gout. Rev Med Suisse 2007;3:720,722-724.
10. Li QI, Wang CN, Song YL. Research progress on NALP3 inflammasome and related diseases. Chin J Conserv Dent (Chin) 2011;21:355-359,328.
11. Zhou Y, Fang L, Jiang L, Wen P, Cao H, He W, et al. Uric acid induces renal inflammation via activating tubular NF-κB signaling pathway. PLoS One 2012;7:e39738.
12. Chen DY, Song ZF, Li F, Zhang DQ. Expression of FOXO1 and FOXO3α on peripheral blood mononuclear cells and their clinical roles in patients with systemic lupus erythemtosus. Chin J Rheumatol (Chin) 2008;12:629-631.
13. Hwang JW, Rajendrasozhan S, Yao H, Chung S, Sundar IK, Huyck HL, et al. FOXO3 deficiency leads to increased susceptibility to cigarette smoke-induced inflammation, airspace enlargement, and chronic obstructive pulmonary disease. J Immunol 2011;187:987-998.
14. Qiu H, Chen C, Wang RL, Luo H, Zhao BX. Progressive chronic inflammatory reaction in spleens of FoxO3a gene knockout mice. Chin J Biol (Chin) 2012;25:1650-1652,1657.
15. Lin L, Hron JD, Peng SL. Regulation of NF-kappaB, Th activation, and autoinflammation by the forkhead transcription factor Foxo3α. Immunity 2004;21:203-213.
16. Im J, Hergert P, Nho RS. Reduced FoxO3a expression causes low autophagy in idiopathic pulmonary fibrosis fibroblasts on collagen matrices. Am J Physiol Lung Cell Mol Physiol 2015;309:L552-L561.
17. Togher S, Larange A, Schoenberger SP, Feau S. FoxO3 is a negative regulator of primary CD8+ T-cell expansion but not of memory formation. Immunol Cell Biol 2015;93:120-125.
18. Tikhanovich I, Kuravi S, Campbell RV, Kharbanda KK, Artigues A, Villar MT, et al. Regulation of FOXO3 by phosphorylation and methylation in hepatitis C virus infection and alcohol exposure. Hepatology 2014;59:58-70.
19. Xuan LL, Hou Q. Recent advances in the study of AMPK and inflammatory pulmonary disease. Acta Pharm Sin (Chin) 2014;49:1089-1096.

(Accepted October 18, 2017; First Online December 28, 2017)
Edited by YUAN Lin